

SUPPORTING INFORMATION TO

On the Mechanism of Iridium-Catalyzed Asymmetric Hydrogenation of Imines and Alkenes: A Theoretical Study

Kathrin H. Hopmann^{a,b,*}, Annette Bayer^a

^a *Department of Chemistry, University of Tromsø, N-9037 Tromsø, Norway*

^b *Centre for Theoretical and Computational Chemistry, University of Tromsø, N-9037 Tromsø, Norway*

* Correspondence email: kathrin.hopmann@uit.no

Table S1 Computed energies for Mechanism A, B and C with B3LYP*.

Table S2 Comparison of barriers for Mechanism A, B and C with dispersion corrections.

Table S3 Computed enthalpies for hydrogenation of **S2** with different substrate orientations

Table S4 Computed barriers for hydrogenation of **S2** with dispersion corrections.

Table S5 Computed energies for Mechanism A1_{IM} and A2_{IM}

Table S6 Computed energies for Mechanism B1_{IM} and C1_{IM}

Table S7 Computed energies for Mechanism B2_{IM} and C2_{IM}

Table S8 Computed energies for Mechanism H1_{IM} and H2_{IM}

Table S9 Computed energies for Mechanism H3_{IM} with H₂ as apical ligand

Table S10 Computed energies for hydrogenation of **S3** with different substrate orientations

Table S11 Computed energies for hydrogenation of **S3** with dispersion corrections

Figure S1 Optimized geometries for Mechanism A

Figure S2 Optimized geometries for Mechanism B

Figure S3 Optimized geometries for Mechanism C

Figure S4 Computed enthalpies for Mechanism A, B and C

Figure S5 Optimized geometries for Mechanism A1_{IM}

Figure S6 Optimized geometries for Mechanism A2_{IM}

Figure S7 Optimized geometries for Mechanism B1_{IM}

Figure S8 Optimized geometries for Mechanism B2_{IM}

Figure S9 Optimized geometries for Mechanism C1_{IM}

Figure S10 Optimized geometries for Mechanism C2_{IM}

Figure S11 Optimized geometries for the first part of Mechanism H1_{IM}

Figure S12 Optimized geometries for the second part of Mechanism H1_{IM}

Figure S13 Optimized geometries for the second part of Mechanism H2_{IM}

Figure S14 Optimized geometries for Mechanism H3_{IM} with H₂ as apical ligand

Figure S15 Optimized enantioselective transition states with CH₂Cl₂ or H₂ as apical ligand

Table S1. Comparison of electronic energies (kcal mol⁻¹) for Mechanism A, B and C at the B3LYP and B3LYP* level (B3LYP geometries).

| | ΔE , B3LYP | ΔE , B3LYP* |
|------------------------|--------------------|---------------------|
| Mechanism A | | |
| Reac _{A-si,a} | 0.0 | 0.0 |
| TS1 _A | 22.0 | 21.7 |
| Inter _A | 11.8 | 12.2 |
| TS2 _A | 23.0 | 23.3 |
| Alkane _A | 22.2 | 23.0 |
| Mechanism B | | |
| Reac _{B-si,b} | -1.6 | -2.2 |
| TS1 _B | 11.3 | 10.6 |
| Inter _B | 5.5 | 4.7 |
| TS2 _B | 6.6 | 5.9 |
| Alkane _B | -5.9 | -5.1 |
| Mechanism C | | |
| Reac _{B-si,b} | -1.6 | -2.2 |
| TS1 _C | 14.7 | 13.4 |
| Inter _C | 14.0 | 12.8 |
| TS2 _C | 15.0 | 13.9 |
| Alkane _C | -5.9 | -5.1 |

Table S2. Comparison of Gibbs free energies (B3LYP) for Mechanism A, B and C with and without empirical dispersion corrections (DFT-D3).

| | $\Delta G^{298K,sol}$ | $\Delta G^{298K,sol,dis}$ |
|---------------------------------|-----------------------|---------------------------|
| Mechanism A | | |
| Reac _{A-si,a} | 0.0 | 0.0 |
| TS1 _A | 19.2 | 23.0 |
| Inter _A | 12.0 | 15.3 |
| TS2 _A | 24.0 | 27.4 |
| Alkane _A | 24.0 | 27.9 |
| η^2 -Alkane _A | 15.6 | 18.6 |
| Mechanism B | | |
| Reac _{B-si,b} | 6.6 | 5.7 |
| TS1 _B | 18.6 | 18.5 |
| Inter _B | 15.7 | 16.1 |
| TS2 _B | 16.2 | 16.9 |
| Alkane _B | 5.2 | 9.6 |
| η^2 -Alkane _B | -5.7 | -1.4 |
| Mechanism C | | |
| Reac _{B-si,b} | 6.6 | 5.7 |
| TS1 _C | 22.7 | 22.0 |
| Inter _C | 22.6 | 21.8 |
| TS2 _C | 23.2 | 22.3 |
| Alkane _{B/C} | 5.2 | 9.6 |
| η^2 -Alkane _{B/C} | -5.7 | -1.4 |

Table S3. Computed enthalpies (kcal mol⁻¹, 298 K, including solvent correction) for hydrogenation of substrate **S2** (catalyst **C1**) with different substrate orientations (Mechanism B).^a

| | Coordination through <i>si</i> -face | | | | Coordination through <i>re</i> -face | | | |
|---------------|--------------------------------------|--------------|--------------|--------------|--------------------------------------|--------------|--------------|--------------|
| | 1si,b | 1si,a | 2si,b | 2si,a | 1re,b | 1re,a | 2re,b | 2re,a |
| Reac | -0.3 | -0.3 | 1.8 | 2.1 | 0.7 | 3.3 | 1.4 | 3.2 |
| TS1 | 10.1 | 14.3 | 15.7 | 18.1 | 14.1 | 20.5 | 12.3 | 15.9 |
| Inter | 7.6 | 11.3 | 11.1 | 17.1 | 12.2 | 15.9 | 9.4 | 12.1 |
| TS2 | 8.0 | 11.8 | 11.3 | 16.6 | 12.6 | 16.1 | 9.8 | 12.7 |
| Alkane | -0.2 | -1.5 | -0.1 | -4.1 | -0.1 | -2.8 | 0.6 | -4.9 |
| Configuration | (<i>R</i>) | (<i>R</i>) | (<i>R</i>) | (<i>R</i>) | (<i>S</i>) | (<i>S</i>) | (<i>S</i>) | (<i>S</i>) |

^a The energetic reference is the **S2**-coordinated dihydride reactant (one hydride above, one equatorial) + free H₂.

Table S4 Comparison of Gibbs free energy barriers (B3LYP) for the hydrogenation of substrate **S2** (with different substrate orientations) with and without empirical dispersion corrections (DFT-D3).

| Coordination | $\Delta G^{298K,sol}$ | $\Delta G^{298K,sol,dis}$ |
|--------------|-----------------------|---------------------------|
| 1si,b | 18.2 | 18.2 |
| 1si,a | 22.6 | 21.4 |
| 2si,b | 23.6 | 24.2 |
| 2si,a | 27.0 | 25.9 |
| 1re,b | 23.2 | 21.6 |
| 1re,a | 28.9 | 29.3 |
| 2re,b | 21.7 | 20.4 |
| 2re,a | 24.1 | 24.4 |

Table S5. Computed energies (kcal mol⁻¹) for Mechanism A1_{IM} and A2_{IM} (Figure S5 and S6, Scheme 6, Substrate **S3** and catalyst **C1**).

| | ΔE | ΔG^{298K} | $\Delta H^{298K,sol}$ | $\Delta G^{298K,sol}$ |
|---------------------------------------|------------|-------------------|-----------------------|-----------------------|
| Reac _{A-IM} | 0.0 | 0.0 | 0.0 | 0.0 |
| TS1 _{A1-IM} | 32.2 | 30.1 | 30.8 | 30.5 |
| Inter _{A1-IM} | 29.4 | 29.4 | 30.0 | 29.7 |
| TS2 _{A1-IM} | 56.0 | 54.3 | 56.2 | 55.9 |
| (<i>R</i>)-Prod _{A1/A2-IM} | 21.8 | 24.6 | 27.3 | 26.8 |
| TS1 _{A2-IM} | 53.6 | 50.5 | 52.2 | 51.3 |
| Inter2 _{A2-IM} | 13.1 | 15.3 | 14.6 | 15.9 |
| TS2 _{A2-IM} | 24.2 | 24.2 | 26.8 | 26.1 |

^a Includes effect of CH₂Cl₂ solvent.**Table S6.** Computed energies (kcal mol⁻¹) for Mechanism B1_{IM} and C1_{IM} (Figure S7 and S9, Scheme 6, Substrate **S3** and catalyst **C1**).^a

| | ΔE | ΔG^{298K} | $\Delta H^{298K,sol\ b}$ | $\Delta G^{298K,sol\ b}$ |
|---------------------------------------|------------|-------------------|--------------------------|--------------------------|
| Reac _{IM,b} | -1.6 | 8.3 | 1.1 | 8.4 |
| TS1 _{B1-IM} | 29.5 | 40.0 | 27.9 | 37.4 |
| Inter _{B1/C1-IM} | 23.2 | 35.2 | 23.3 | 31.8 |
| TS2 _{B1/C1-IM} | 32.6 | 44.6 | 34.7 | 43.5 |
| (<i>S</i>)-Prod _{B1/C1-IM} | -9.9 | 4.8 | -3.4 | 3.9 |
| Reac _{IM,a} | -0.2 | 10.8 | 1.4 | 9.6 |
| TS1 _{C1-IM} | 40.8 | 50.5 | 38.4 | 47.8 |

^a The energetic reference is Reac_{A-IM} + free H₂. ^b Includes effect of CH₂Cl₂ solvent.**Table S7.** Computed energies (kcal mol⁻¹) for Mechanism B2_{IM} and C2_{IM} (Figure S8 and S10, Scheme 6, substrate **S3** and catalyst **C1**).^a

| | ΔE | ΔG^{298K} | $\Delta H^{298K,sol\ b}$ | $\Delta G^{298K,sol\ b}$ |
|------------------------------------|------------|-------------------|--------------------------|--------------------------|
| Reac _{IM,a} | -0.2 | 10.8 | 1.4 | 9.6 |
| TS1 _{B2-IM} | 50.5 | 60.0 | 48.1 | 57.5 |
| Inter _{B2-IM} | 7.4 | 22.5 | 11.0 | 20.9 |
| TS2 _{B2-IM} | 12.6 | 27.0 | 15.2 | 25.6 |
| (<i>S</i>)-Prod _{B2-IM} | -13.6 | 1.9 | 1.2 | -6.9 |
| Reac _{IM,b} | -1.6 | 8.3 | 1.1 | 8.4 |
| TS1 _{C2-IM} | 41.4 | 51.6 | 40.0 | 49.9 |
| Inter _{C2-IM} | 8.8 | 23.1 | 11.5 | 21.3 |
| TS2 _{C2-IM} | 11.9 | 25.8 | 13.9 | 24.1 |
| (<i>S</i>)-Prod _{C2-IM} | -16.2 | -0.1 | -9.5 | -0.8 |

^a The energetic reference is Reac_{A-IM} + free H₂. ^b Includes effect of CH₂Cl₂ solvent.

Table S8. Computed energies (kcal mol⁻¹) for Mechanism H1_{IM} and H2_{IM} (Figure S11-S13, Scheme 7, substrate **S3** and catalyst **C1**).^a

| | ΔE | ΔG^{298K} | $\Delta H^{298K, \text{sol b}}$ | $\Delta G^{298K, \text{sol b}}$ |
|---|------------|-------------------|---------------------------------|---------------------------------|
| Reac _{IM,b} | -1.6 | 8.3 | 1.1 | 8.4 |
| TS1 _{H1/H2-IM} | 24.6 | 31.7 | 23.9 | 30.8 |
| Inter1 _{H1/H2-IM} | 22.4 | 31.5 | 22.4 | 28.9 |
| Inter2 _{H1/H2-IM} | 9.7 | 15.9 | 13.3 | 15.6 |
| TS2 _{H1-IM} | 25.3 | 35.7 | 25.7 | 32.8 |
| Inter3 _{H1-IM} | 4.7 | 20.2 | 7.6 | 17.9 |
| TS2 _{H1-IM} | 11.3 | 25.3 | 15.5 | 23.2 |
| (<i>R</i>)-Prod _{H1-IM} | -0.9 | 13.7 | 6.4 | 13.0 |
| TS2 _{H2-IM} | 17.0 | 29.2 | 16.7 | 25.4 |
| (<i>R</i>)-Prod _{H2-IM} | 8.7 | 21.5 | 11.5 | 18.5 |
| (<i>R</i>)-Prod _{H2-IM-H2 bound} | -16.9 | -4.8 | -14.4 | -5.9 |

^a The energetic reference is Reac_{A-IM} + free H₂. ^b Includes effect of CH₂Cl₂ solvent.**Table S9.** Computed energies (kcal mol⁻¹) for Mechanism H3_{IM} with H₂ as additional ligand (Figure S14, Scheme 7, Substrate **S3** and catalyst **C1**).

| | Electronic Energy | ΔG^{298K} | $\Delta H^{298K, \text{sol a}}$ | $\Delta G^{298K, \text{sol a}}$ |
|--------------------------------|-------------------|-------------------|---------------------------------|---------------------------------|
| Reac _{IM,b} | 0.0 | 0.0 | 0.0 | 0.0 |
| Inter1 _{H3-IM,H2} | 5.7 | 12.0 | 8.9 | 13.0 |
| TS1 _{H3-IM,H2} | 8.0 | 13.6 | 10.2 | 15.2 |
| Inter2 _{H3-IM,H2} | -2.9 | 5.7 | -0.1 | 4.5 |
| TS2 _{H3-IM,H2} | 8.5 | 19.4 | 9.6 | 17.7 |
| Prod _{H3-IM} | -0.8 | 11.9 | 3.0 | 10.5 |
| Prod _{H3-IM-bound,H2} | -18.1 | -1.9 | -13.4 | -4.5 |

^a Includes solvent effects.**Table S10.** Computed Energies (kcal mol⁻¹) for hydrogenation of substrate **S3** (catalyst **C1**) with different substrate orientations at TS2 (Mechanism H_{IM}, H₂ above, Figure S15).^a

| Orientation | Electronic | ΔG^{298K} | $\Delta H^{298K, \text{sol b}}$ | $\Delta G^{298K, \text{sol b}}$ | Configuration |
|-------------------------|------------|-------------------|---------------------------------|---------------------------------|---------------|
| 1re_{IM} | 8.8 | 19.6 | 11.1 | 17.8 | (<i>S</i>) |
| 2re_{IM} | 9.8 | 20.3 | 12.1 | 18.6 | (<i>S</i>) |
| 1si_{IM} | 8.5 | 19.4 | 10.8 | 17.7 | (<i>R</i>) |
| 2si_{IM} | 8.5 | 20.1 | 10.4 | 17.7 | (<i>R</i>) |

^a Reac_{IM,b} (with free H₂) as energetic reference, ^b Includes solvent effect..

Table S11. Computed Gibbs Free barriers (kcal mol⁻¹) for hydrogenation of substrate **S3** (catalyst **C1**) with different substrate orientations at TS2 (Mechanism H_{IM}, CH₂Cl₂ above, Figure S15) with and with dispersion corrections (DFT-D3).^a

| Orientation | $\Delta G^{298\text{K},\text{sol}}$ ^b | $\Delta G^{298\text{K},\text{sol},\text{dis}}$ ^b | Configuration |
|-------------------------|--|---|---------------|
| 1re_{IM} | 19.4 | 23.2 | (<i>S</i>) |
| 2re_{IM} | 19.5 | 23.8 | (<i>S</i>) |
| 1si_{IM} | 17.7 | 21.2 | (<i>R</i>) |
| 2si_{IM} | 18.1 | 22.6 | (<i>R</i>) |

^a Reac_{IM,,b} (with free H₂) as energetic reference, ^bIncludes solvent effect..

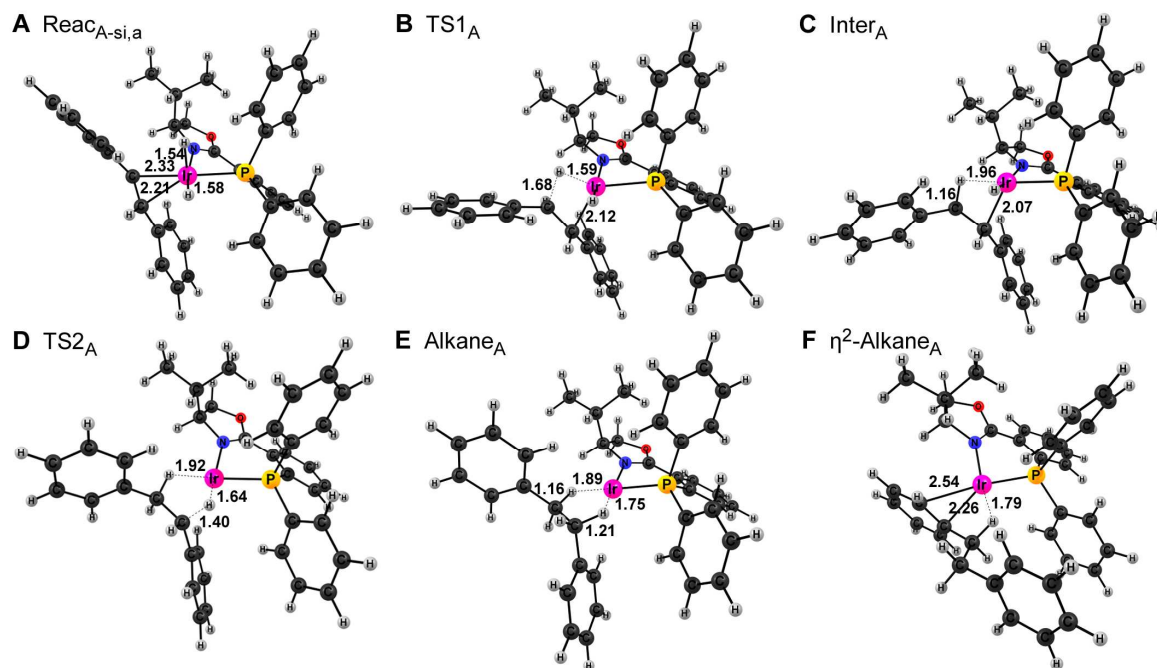


Figure S1. Optimized geometries for Mechanism A (catalyst **C1**, substrate **S1**), **A**) $\text{Reac}_{\text{A-si,a}}$, **B**) TS1_A , **C**) Inter_A , **D**) TS2_A , **E**) Alkane_A , **F**) $\eta^2\text{-Alkane}_\text{A}$.

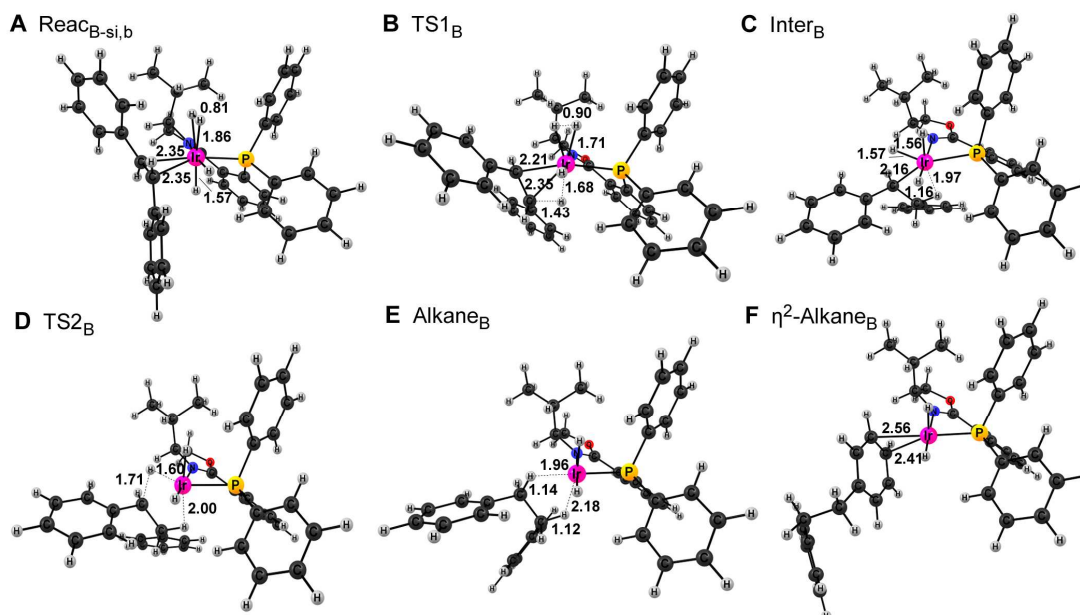


Figure S2. Optimized geometries for Mechanism B (catalyst **C1**, substrate **S1**), **A**) $\text{Reac}_{\text{B-si,b}}$, **B**) TS_B , **C**) Inter_B , **D**) TS2_B , **E**) Alkane_B , **F**) $\eta^2\text{-Alkane}_\text{B}$.

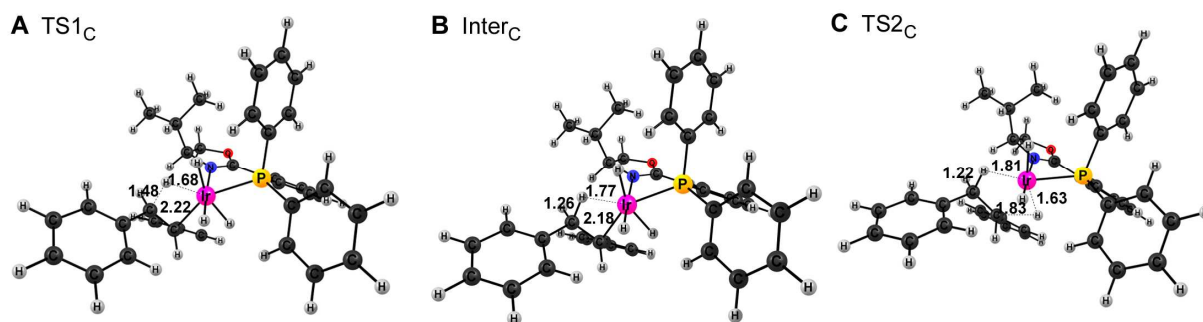


Figure S3. Optimized geometries for Mechanism C (C1 and S1), A) TS1_C, B) Inter_C, C) TS2_C.

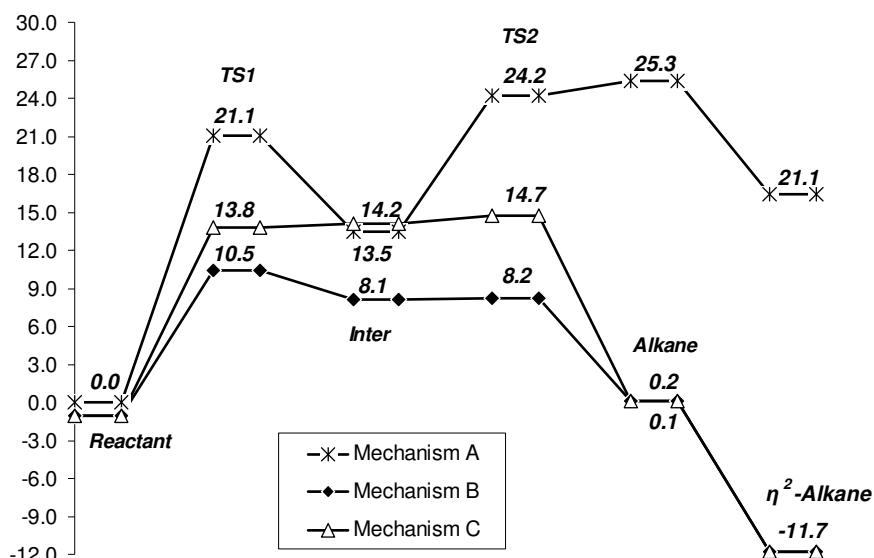


Figure S4. Computed enthalpies (kcal mol⁻¹, corrected for solvent effects) for Mechanism A, B and C (catalyst C1 and substrate S1).

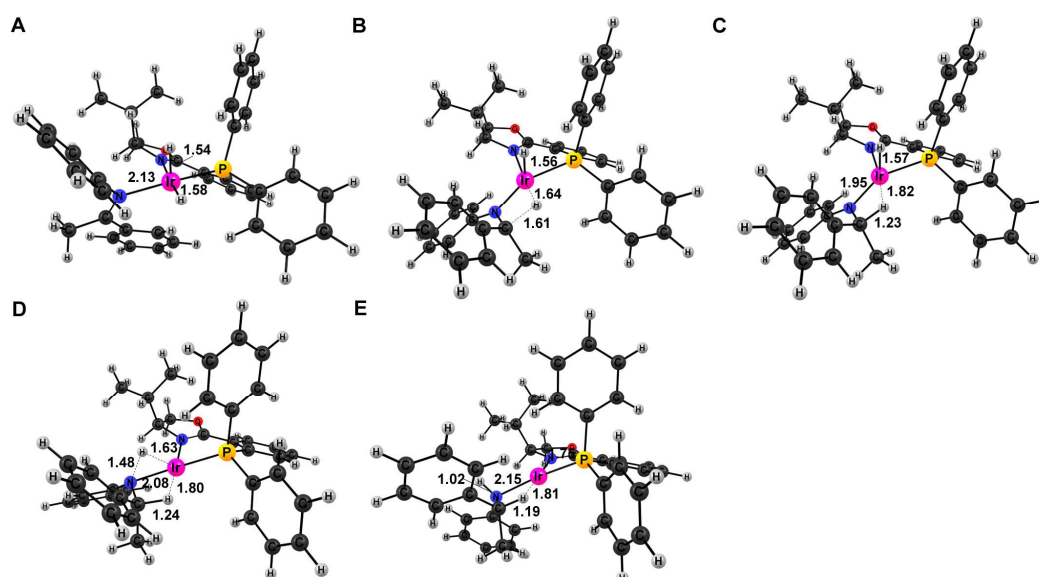


Figure S5. Optimized geometries for Mechanism A1_{IM} (catalyst C1, substrate S3). A) React_{A-IM}, B) TS1_{A1-IM}, C) Inter_{A1-IM}, D) TS2_{A1-IM}, E) (*R*)-Prod_{A1-IM}.

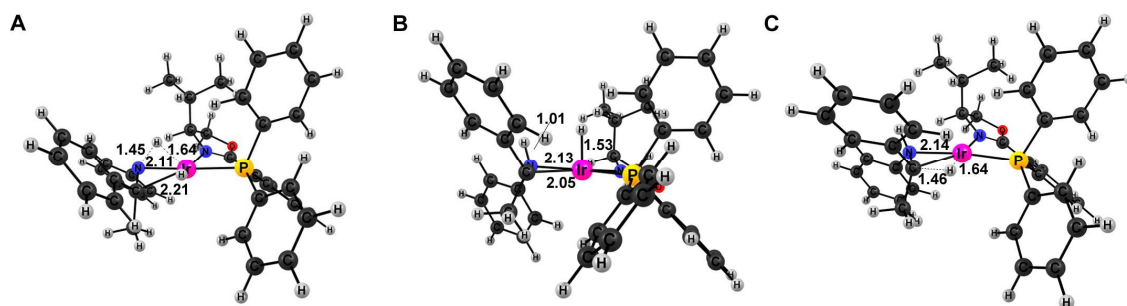


Figure S6. Optimized geometries for Mechanism A2_{IM} (catalyst C1, substrate S3). A) TS1_{A2-IM}, B) Inter_{A2-IM}, C) TS2_{A2-IM}.

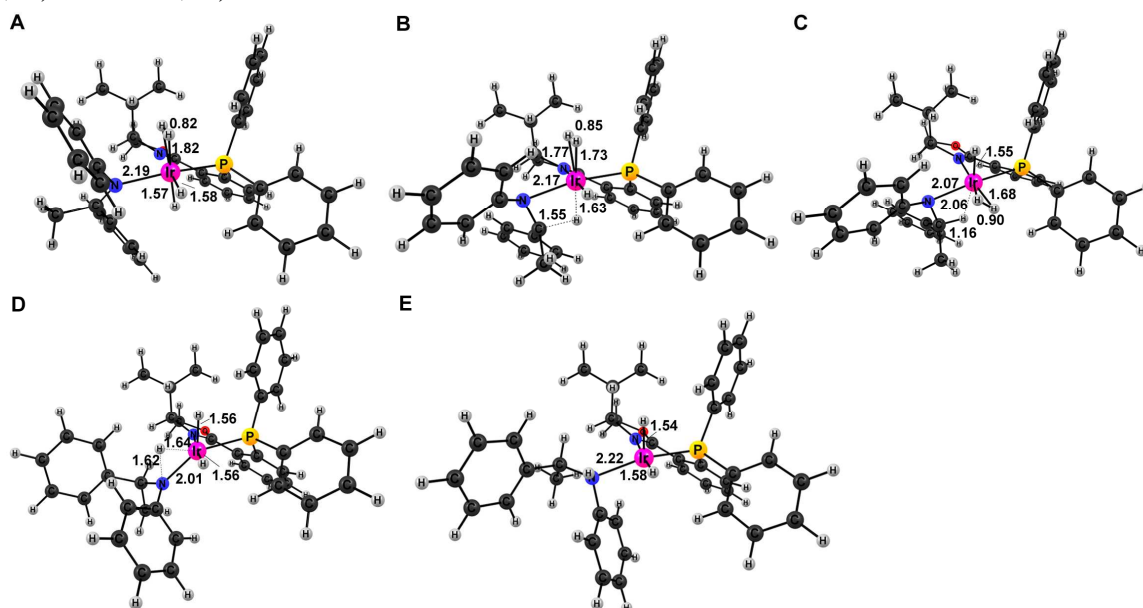


Figure S7. Optimized geometries for Mechanism B1_{IM} (catalyst C1, substrate S3). A) Reac_{IM,b}, B) TS1_{B1-IM}, C) Inter_{B1/C1-IM}, D) TS2_{B1/C1-IM}, E) (S)-Prod_{B1/C1-IM}.

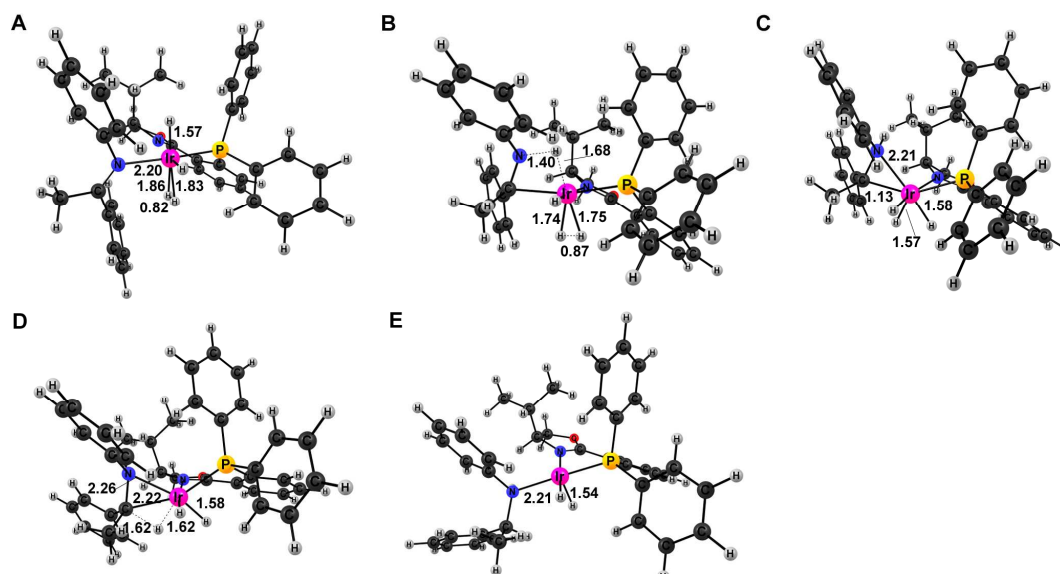


Figure S8. Optimized geometries for Mechanism B2_{IM} (catalyst C1, substrate S3). A) Reac_{B2-IM}, B) TS1_{B2-IM}, C) Inter_{B2-IM}, D) TS2_{B2-IM}, E) Prod_{B2-IM}.

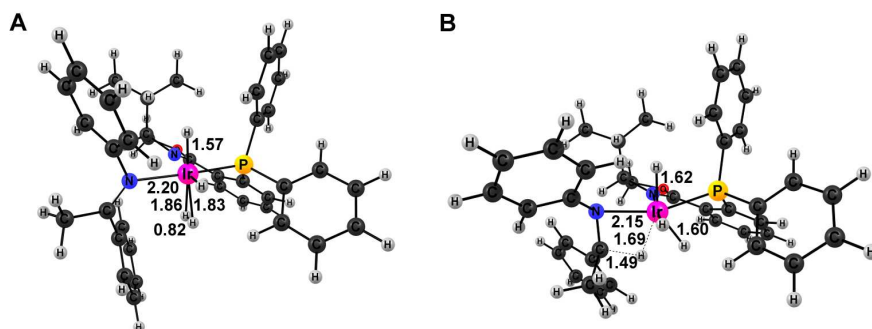


Figure S9. Optimized geometries for Mechanism C1_{IM} (C1 and S3). A) React_{IM,a}, B) TS1_{C1-IM}. The remaining reaction occurs as for Mechanism B1_{IM} (Figure S8).

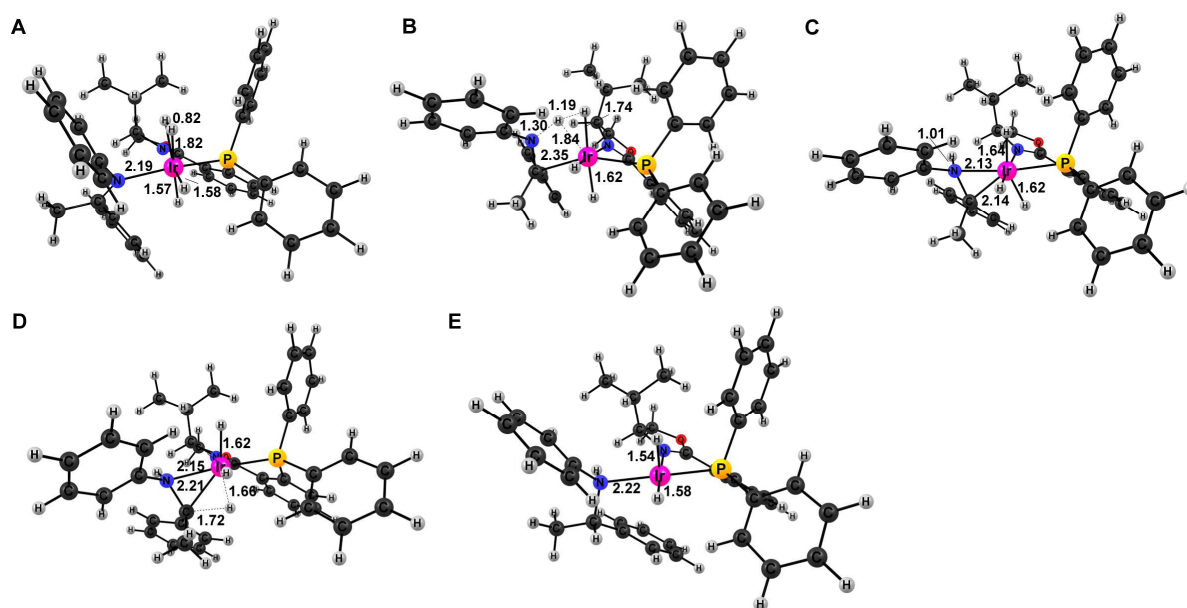


Figure S10. Optimized geometries for Mechanism C2_{IM} (catalyst C1, substrate S3). A) React_{C2-IM}, B) TS1_{C2-IM}, C) Inter_{C2-IM}, D) TS2_{C2-IM}, E) Prod_{C2-IM}.

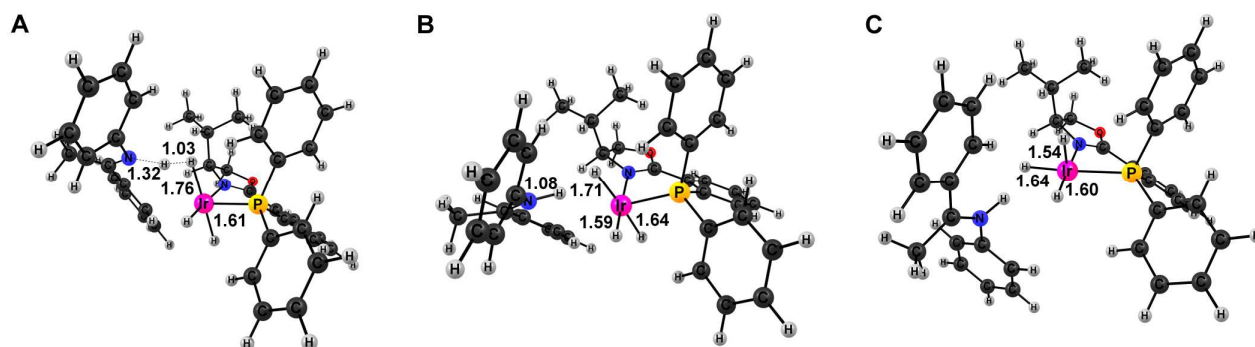


Figure S11. Optimized geometries for the first part of Mechanism H1_{IM} (catalyst C1, substrate S3). A) React_{H1-IM}, B) TS1_{H1-IM}, C) Inter1_{H1-IM}.

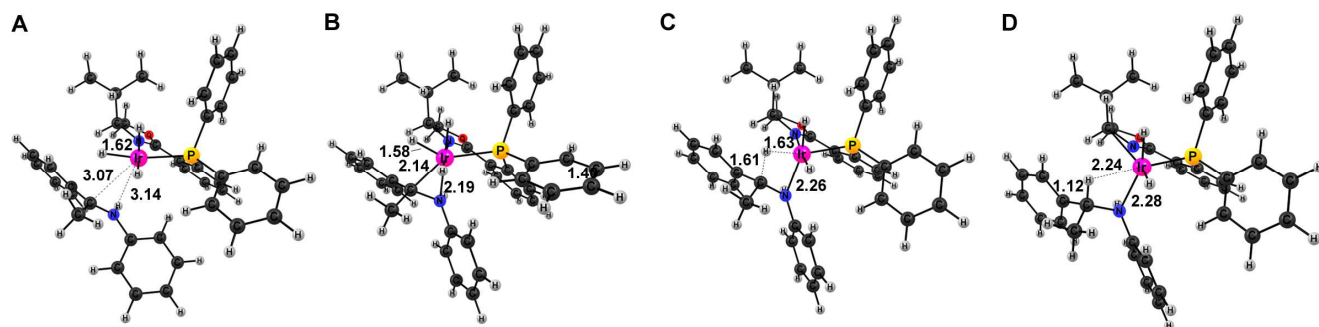


Figure S12. Optimized geometries for the second part of Mechanism H1_{IM} (catalyst C1, substrate S3). **A)** TS_{2H1-IM}, **B)** Inter_{3H1-IM}, **C)** TS_{2H1-IM}, **D)** Prod_{H1-IM}.

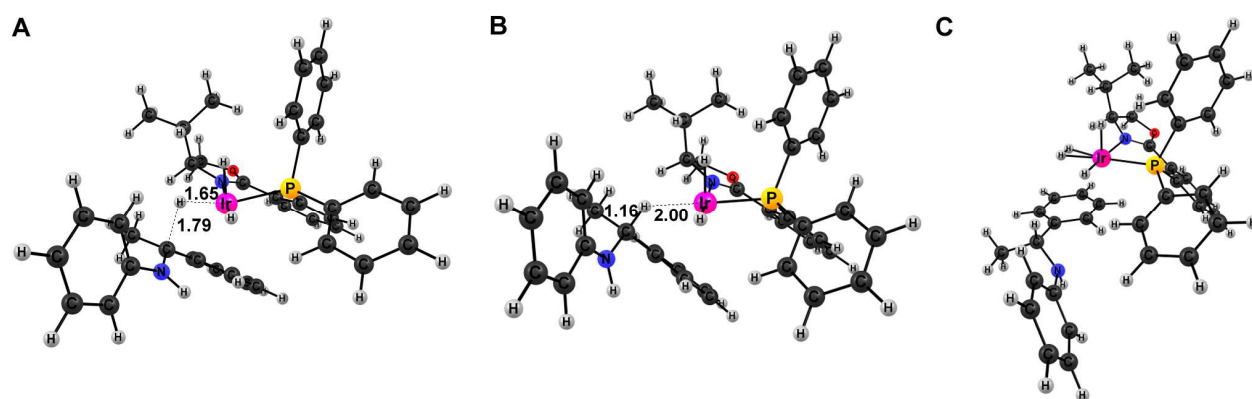


Figure S13. Optimized geometries for the second part of Mechanism H2_{IM} (catalyst C1, substrate S3). **A)** TS_{2H2-IM}, **B)** Prod_{H2-IM}, **C)** Prod_{H2-IM-H2} bound.

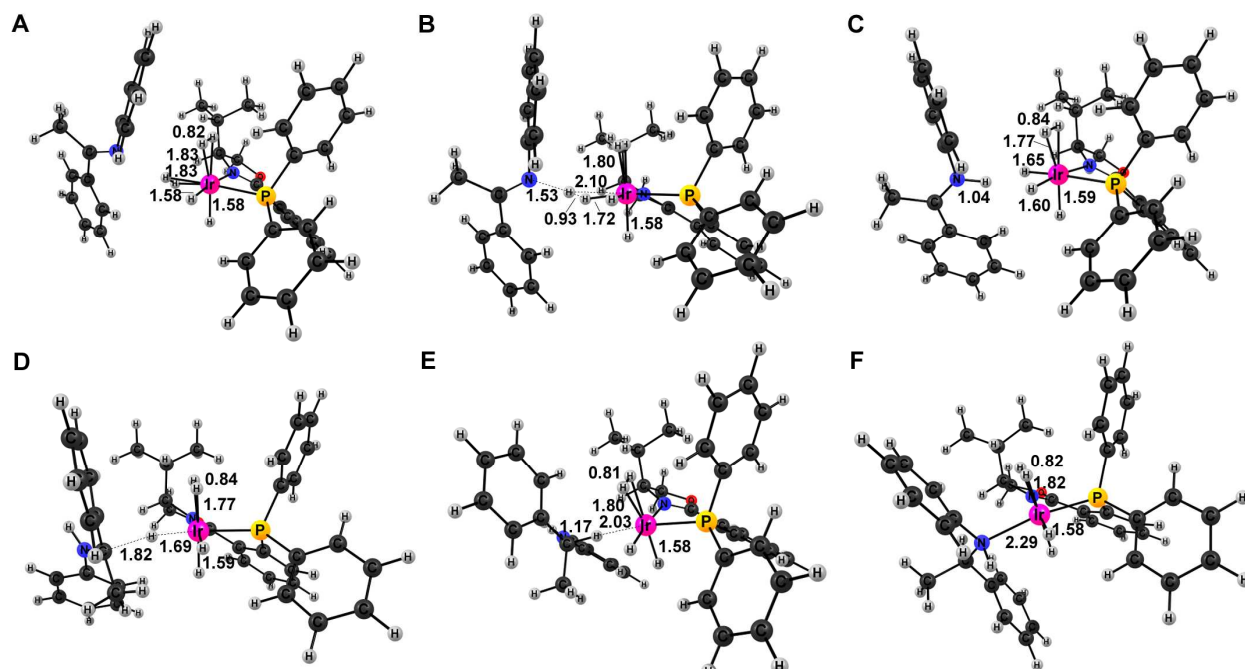


Figure S14. Optimized geometries for Mechanism H3_{IM} with H₂ as ligand (catalyst C1 and substrate S3). **A)** Reac_{H3-IM,H2}, **B)** Inter_{1H3-IM,H2}, **C)** TS_{1H3-IM,H2}, **D)** Inter_{2H3-IM,H2}, **E)** TS_{2H3-IM,H2}, **F)** (R)-Prod_{H3-IM,H2}, **G)** (R)-Prod_{H3-IM-bound,H2}.

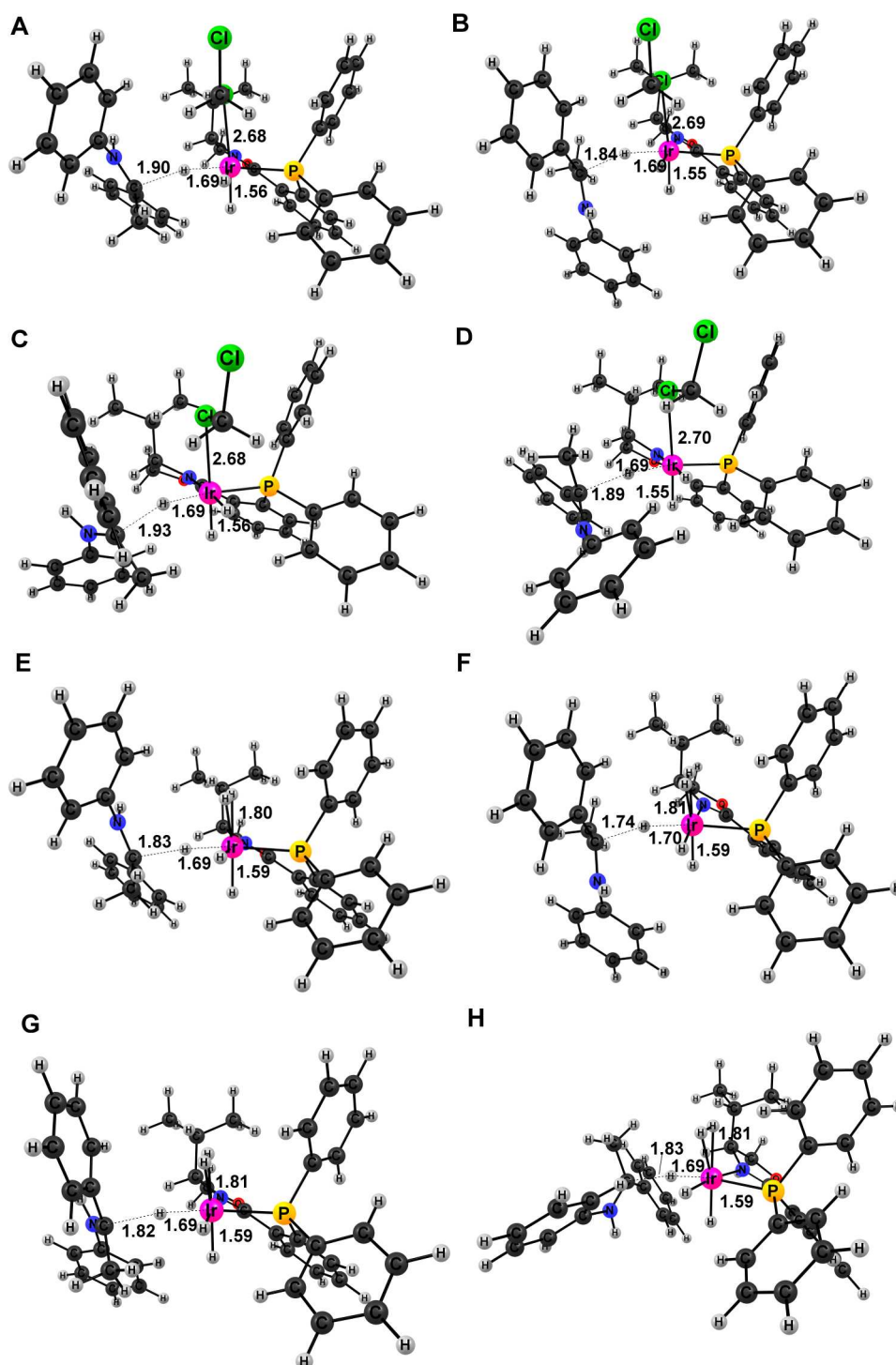


Figure S15. Optimized transition states for hydride transfer to the free iminium with CH_2Cl_2 (A-D) or H_2 (E-H) as apical ligand. A) 1re_{IM} (CH_2Cl_2), B) 2re_{IM} (CH_2Cl_2), C) 1si_{IM} (CH_2Cl_2), D) 2si_{IM} (CH_2Cl_2), E) 1re_{IM} (H_2), F) 2re_{IM} (H_2), G) 1si_{IM} (H_2), H) 2si_{IM} (H_2).